On the Use of Mobile Power Sources in Distribution Networks under Endogenous Uncertainty

Jinshun Su, *Student Member, IEEE,* Dmitry Anokhin, Payman Dehghanian, *Senior Member, IEEE,* and Miguel A. Lejeune

***Abstract*—Mobile power sources (MPSs) have promising potential for spatiotemporal flexibility exchange in power distribution systems (DS). They can be strategically employed to enhance the network resilience when facing the aftermath of high-impact low-probability (HILP) events. This paper proposes a novel service restoration formulation that models and accounts for the endogenous uncertainty in the MPSs routing and scheduling decision making. The proposed restoration model is formulated as a mixed-integer nonlinear programming (MINLP) problem with nonconvex continuous relaxation. We derive computationally tractable linearization procedures to reformulate the MINLP model as an equivalent mixed-integer linear programming (MILP) problem. Case studies on the IEEE 33-node and 123-node test systems demonstrate the role of incorporating endogenous uncertainties in the decision-making process and the effectiveness of the proposed restoration scheme in boosting the DS resilience.**

***Index Terms*—Endogenous uncertainty; power distribution system (DS); high-impact low-probability (HILP) events; mobile power sources (MPSs); resilience.**

NOMENCLATURE

A. Sets and Indices

$i, j \in \mathbf{B}$	Index and set of nodes in the network.
$m \in \mathbf{M}$	Index and set of mobile power sources (MPSs).
$l(i,j) \in \mathbf{L}$	Index and set of network branches.
$k \in \mathbf{K}$	Index and set of MPS stations.
$\mathbf{L^d} \in \mathbf{L}$	Subset of damaged branches in the network.
$\mathbf{L^s} \in \mathbf{L}$	Subset of branches that are equipped with remotely-controlled switches (RCSs).
$\mathbf{B^s} \in \mathbf{B}$	Subset of nodes that are selected as sources of fictitious supply in a physical island.

B. Parameters and Constants

α_i	Value of restored load at node i (\$/kW).
δ_m	Generation cost coefficient of MPS m (\$/kW).
C_{ik}	Operation cost coefficient for MPSs to reach node i from station k (\$).
P_i^0	Survived demand after an HILP event (kW).
Ψ_m^+, Ψ_m^-	Maximum real and reactive power output of MPS m (kW, kVar).
N	Number of nodes in the network.
N^i	Number of physical islands formed due to damaged and un-repaired branches in the network.
M^f, M^s	Big M numbers denoting maximum value of fictitious power flow and fictitious supply.
d_i^f	Fictitious load of node i.
M^v	Big M number denoting maximum value of the difference in the squared voltage magnitudes.
$\overline{P}_i^d, \overline{Q}_i^d$	Maximum real and reactive power demand at node i (kW, kVar).
$\overline{P}_l, \overline{Q}_l$	Real and reactive power capacity of branch l (kW, kVar).
$\overline{P}^g, \overline{Q}^g$	Maximum real and reactive power output of the substation node (kW, kVar).
$\underline{P}^g, \underline{Q}^g$	Minimum real and reactive power output of the substation node (kW, kVar).
$\underline{V}_i^s, \overline{V}_i^s$	Minimum and maximum squared voltage magnitude at node i (kV^2).
T_{ik}	MPS travel time to node i from station k (p.u.).
M_{mk}	Big M number representing the maximum number of trips for MPS m at station k.
c_k	Maximum number of MPSs that can be hosted by station k.
τ_{mi}	Service time of node i served by MPS m (p.u.).
R_l, X_l	Resistance and reactance of branch l (Ω).

C. Decision Variables

ψ_m^+, ψ_m^-	Real and reactive power of MPS m (kW, kVar).
f_l	Fictitious flow on branch l.
f_i^g	Fictitious supply at source node i.
p_l^f, q_l^f	Real and reactive power flow on branch l (kW, kVar).
p_i^d, q_i^d	Final real and reactive demand at node i following the restoration process (kW, kVar).
p_i^g, q_i^g	Real and reactive power generation from stationary generating units at node i (kW, kVar).
p_i, q_i	Total real and reactive power output of MPSs at node i (kW, kVar).
V_i^s	Squared voltage magnitude at node i (kV^2).
r_i	Immediate restoration metric (IRM) of node i.
w_i	Waiting time for node i served by MPSs (p.u.).
v_{mki}	Variable representing waiting time for node i to be served by MPS m from station k (p.u.).
t_i	Travel time for MPSs to reach node i (p.u.).
λ_l	Binary variable defining the status of branch l: = 1 if the branch is connected, = 0 otherwise.
μ_{mki}	Binary variable for the assignment of an MPS: = 1 if node i is served by MPS m originally located at station k, = 0 otherwise.
y_{mk}	Binary variable for the location of an MPS: =1 if MPS m is located at station k, = 0 otherwise.

This work is supported in part by the National Science Foundation (NSF) grants ECCS-2114100 and RISE-2220626, and the Office of Naval Research (ONR) grant N00014-22-1-2649.

J. Su and P. Dehghanian are with the Department of Electrical and Computer Engineering, George Washington University, Washington, DC 20052, USA (e-mails: jsu66@gwu.edu; payman@gwu.edu).

D. Anokhin and M. A. Lejeune are with the Department of Decision Sciences, George Washington University, Washington, DC 20052, USA (e-mails: danokhin@gwu.edu; mlejeune@gwu.edu).

I. INTRODUCTION

A. Motivation and Rationale

THE more frequent occurrence of high-impact low-probability (HILP) incidents—e.g., hurricanes, floods, earthquakes, wildfires—has recently led to large-scale long-lasting power outages. The resulting tremendous economic losses and significant disruptions in our society have highlighted the importance and urgency to enhance power grid resilience to such extremes. Mobile power sources (MPSs) are emergency service vehicles that can offer spatio-temporal flexibility to enhance the power distribution system (DS) resilience [1]. MPSs can be effective resources when sustained damage leads to prolonged electric service outages in DS. However, they are currently not well utilized in practice. For example, before Hurricane Sandy struck, 400 industrial-size MPSs were prepared by the Federal Emergency Management Agency, but only a portion of them was providing power three days after Sandy made its landfall [2]. Holistic strategies to enhance the efficiency of the MPSs utilization can render faster restoration and augmented resilience.

B. Literature Review

Research on the deployment of MPSs in response to devastating extremes has been conducted over the past decade. The study in [3] proposed a two-stage restoration scheme for DS restoration with a mixed-integer linear programming (MILP) model. The scheme highlighted the full potential of MPSs dispatch jointly with the dynamic DS reconfiguration. A post-disaster restoration scheme presented in [4] could enhance the DS resilience by scheduling MPSs in coordination with DS reconfiguration. A rolling integrated service restoration strategy for scheduling and routing MPSs is introduced in [5], capturing the uncertainty in the status of the roads and electric branches. A co-optimization approach formulated as a mixed-integer second-order cone programming model is introduced in [6] that coordinates the MPSs and repair crews dispatch for DS resilience. The study in [7] proposed a temporal-spatial status model with an MILP formulation for MPS deployment in unbalanced DS. The study in [1] proposed a two-stage robust optimization model for resilient scheduling and routing of MPSs considering an optimal pre-positioning strategy. A two-stage dispatch framework for pre-positioning and real-time allocation of MPSs is introduced in [8], where a scenario-based two-stage stochastic optimization model is formulated for strengthening the DS resilience. The study in [9] presents a multi-agent approach for service restoration with MPSs participation, where the cyber, physical, and transportation constraints are taken into account. A joint post-disaster restoration scheme applying MPSs and distributed generators tackling the transportation system constraints is proposed in [10]. A framework is presented in [11] to determine the DS restoration strategy considering the dispatch of MPSs and repair crews in the transportation system. The study in [12] proposed a co-optimization model including MPSs, repair crews, and soft-open-point networked microgrids to enhance the DS resilience. A microgrid-based critical service restoration strategy with properly positioning MPSs is introduced in [13].

In [1], [3], [6], [7], [9]–[12], [14], [15], the routing and scheduling of MPSs is approached through multi-period models that specify the decisions for the entire restoration horizon. Such models allow for sequential changes in the network topology, MPSs, and repair crews allocation status, etc. during the DS restoration process. The performance of the multi-period models might, however, be compromised due to the prevailing uncertainties during the restoration process and the need for dynamic information updates in different restoration intervals. Accordingly, a rolling optimization perspective is investigated for MPSs routing and scheduling in [5]. The rolling horizon approach is based on a scheduling formulation that solves iteratively the deterministic problem by moving forward the optimization horizon in each iteration [16] and has been applied to power system problems [17]–[19]. However, the resulting formulations are typically complex and computationally challenging.

State-of-the-art models in the literature on the MPSs allocation and dispatch have been primarily based on the simplifying assumption that MPSs are immediately available during the entire restoration process and that their travel time is the only contributor to the DS response and recovery. To achieve a more realistic restoration model using MPSs, any delays prior to the trip should be captured in the decision-making process, which in turn affect the immediate service restoration of the load points in the DS. Such delays can include the time to decide which MPS to dispatch, the time to contact the MPS, the time for the crew to reach its MPS and commission it, and the travel time for the MPSs to reach the interrupted nodes.

C. Problem Statement and Contributions

In contrast with risk-neutral and risk-averse stochastic programming formulations with exogenous uncertainties, there has been minimal effort so far to formally model sources of endogenous uncertainty in the context of electric power systems operation in general and on service restoration during emergencies in particular. This highlights the need for decision support systems (models and solution algorithms) to intelligently navigate both immediate and gradual uncertainties in energy systems. This paper has explored and contributed to filling these knowledge gaps by providing analytical models representative of the actual decisional context. The situation in which a vehicle's availability is uncertain and depends on its workload, itself determined by its location and assigned tasks, was coined *endogenous uncertainty* [20] in the late 80's. The extant literature on MPS scheduling and dispatch for DS resilience [9]–[15] has ignored the endogenous sources of uncertainty in the decision-making process. However, the waiting time for a request to be served by an MPS is uncertain and depends on the workload of the MPS and its possible non-immediate availability when called upon, which are both affected by other decision variables (e.g., requests assigned to MPS, the location, and dispatch route of the MPS) taken within the optimization model. This illustrates the prevalence of decision-dependent or endogenous uncertainty in the deployment of MPSs for DS resilience.

The main contributions of this paper are as follows

- We present a new service restoration model in the DS via MPSs routing and dispatch scheduling along with possible network topology re-configurations which accounts for endogenous uncertainty in MPSs' availability.
- We propose a mixed-integer non-linear programming (MINLP) optimization model through a single-time pe-

riod framework for boosting DS resilience. A linearization approach is introduced to reformulate the MINLP model to an equivalent and computationally tractable mixed-integer linear programming (MILP) model.
- We empirically evaluate the performance of the proposed optimization approach quantified and compared with traditional MPSs modeling approaches. We numerically demonstrate the effective role of endogenous uncertainties in offering a more realistic estimation of the MPSs contributions to DS resilience enhancement.

The paper is organized as follows. Section II introduces endogenous uncertainty and gives insights on its impact on the DS restoration problem with MPSs. Section III introduces the proposed MPS optimization model with endogenous uncertainty. Section IV describes the method to reformulate the MINLP problem as an equivalent MILP. Several numerical case studies are presented in Section V to validate the proposed model under a variety of outage scenarios, evaluate its scalability and computational efficiency, and compare its performance with the traditional models. Research findings are eventually summarized in Section VI.

II. Endogenous Uncertainty

There are two main types of uncertainties: *exogenous uncertainties* are independent of decisions, while *endogenous uncertainties* or decision-dependent uncertainties [21], [22] are impacted by decisions taken within an optimization problem. Several forms of endogenous uncertainty can be distinguished (see taxonomy in [21]). In models with Type 1 endogenous uncertainty, decisions impact the probability distribution of (some) random variables. Problems with Type 2 endogenous uncertainty are two- or multi-stage stochastic programs with recourse in which decisions affect the time at which information is revealed and the uncertainty gets resolved. A recent review [21] identified other types of endogenous uncertainty involving the concept of busy probability [23]–[25], endogenous uncertainty sets in robust optimization [26], and in distributionally robust optimization [27], [28].

The modeling of the (endogenous) dependency connecting random and decision variables is challenging and often results in the formulation of nonconvex problems. To avoid the inherent modeling and solution challenges, simplifying assumptions are often used. We refer the readers to [20], [23], [24], [29], [30] for a detailed discussion of these simplifications and the issues they cause (i.e., models not representative of the actual problems and questionable decisions). In this study, we propose the immediate restoration metric (IRM) r_i and define it as the probability of an interrupted node i to be served immediately by an MPS, which is determined by other decisions taken within the optimization problem — hence endogenous uncertainty. The IRM depends on the time needed to restore service to the interrupted node: the sum of the travel time t_i for the assigned MPS to reach node i and waiting time w_i for an interrupted node i served by the assigned MPS. Note that the restoration process is impacted by how quickly MPSs serve the interrupted nodes. An interrupted node cannot be restored immediately, if the assigned MPS is not immediately available (or is busy). Hence, we define IRM for the interrupted node i as an endogenous uncertainty which is driven by the *busy probability* of an MPS and the resulting waiting time and delay incurred when using an MPS. Introduced several decades ago in the context of probabilistic location problems [20], *busy probability* is used to model the probabilistic nature of a vehicle's availability. The busy probability is calculated as the ratio of the vehicle's workload to its total service time and is called an endogenous uncertainty (see [20], [23] and the references therein). Several recent studies provide a thorough explanation of the endogenous nature of the availability of vehicles [23], [24] and make a compelling case on the need to endogenize this uncertainty via the concept of busy probability. In the suggested model, the endogenous uncertainty in MPSs' busy probability is reflected and propagates in the proposed IRM metric.

Our optimization model endogenizes and calculates an *individual* IRM for each interrupted node and for each individual MPS assignment. The proposed model does not assume that interrupted nodes have all the same IRM, nor that IRMs are fixed (exogenous) parameters computed ex-ante, prior to solving the optimization model. We define the IRM of interrupted node i as $r_i = 1 - (t_i + w_i)$. The times t_i and w_i are both normalized with respect to the maximum admissible time for restoration and are thus defined on $[0, 1]$, so does the proposed IRM r_i. If the interrupted node i can be served immediately by an MPS, $r_i = 1$. Otherwise, r_i decreases proportionally with the time to restore node i.

The proper modeling of the dependency of the endogenous uncertainties on decisions is modelled with the linking constraints (1a)-(1e) presented next:

$$t_i = \sum_{k\in\mathbf{K}} \sum_{m\in\mathbf{M}} T_{ik}\mu_{mki} \qquad i \in \mathbf{B} \quad (1a)$$

$$v_{mk1} = 0 \qquad k \in \mathbf{K}, m \in \mathbf{M} \quad (1b)$$

$$v_{mki} = \mu_{mki}\left(\sum_{i'=1}^{i-1} \mu_{mki'}(T_{i'k} + \tau_{mi'})\right) \qquad k \in \mathbf{K}, i \in \mathbf{B}\setminus\{1\}, m \in \mathbf{M} \quad (1c)$$

$$w_i = \sum_{m\in\mathbf{M}} \sum_{k\in\mathbf{K}} v_{mki} \qquad i \in \mathbf{B} \quad (1d)$$

$$t_i + w_i \le 1 \qquad i \in \mathbf{B} \quad (1e)$$

Constraint (1a) defines the travel time of MPS m from station k to reach the interrupted node i, where μ_{mki} defines whether node i was served by MPS m located at station k. Constraint (1c) defines the waiting time for MPS m located at station k to serve the interrupted node i. The parameters T_{ik} and τ_{mi} represent the travel time from station k to node i and the service time for node i serviced by MPS m, respectively. The term $\sum_{i'=1}^{i-1} \mu_{mki'}(T_{i'k} + \tau_{mi'})$ in (1c) is the sum of the travel and service times to reach and restore power at all interrupted nodes, except the node served first ($i = 1$), if they were served by MPS m. If node i is serviced by MPS m from station k implying $\mu_{mki} = 1$, then the waiting time takes the value of $\sum_{i'=1}^{i-1} \mu_{mki'}(T_{i'k} + \tau_{mi'})$ and 0 otherwise. Constraint (1d) defines the waiting time to restore power at node i with the MPS selected to serve interrupted node i. Constraint (1e) ensures that service restoration to node i is achieved within the maximum admissible time (i.e., ≤ 1). The power restoration is assumed to be handled in the order in

which outages are notified to the DS operator. This assumption impacts the assessment of the waiting time to serve interrupted node i and affects constraint (1e). Constraint (1b) states that the auxiliary variable v_{mk1} for the node serviced first ($i = 1$) is zero since at least one MPS is available to serve this node.

Expanding the expression $1 - (t_i + w_i)$ using the linking constraints (1a)-(1e), we obtain

$$r_i = 1 - \Big[\sum_{k\in\mathbf{K}} \sum_{m\in\mathbf{M}} T_{ik}\mu_{mki} + \sum_{m\in\mathbf{M}} \sum_{k\in\mathbf{K}} \mu_{mki} \left(\sum_{i'=1}^{i-1} (T_{i'k} + \tau_{mi'})\mu_{mki'} \right) \Big] \quad i \in \mathbf{B} \setminus \{1\} \qquad (2)$$

The above expression shows how the decision variables μ_{mki} defining the MPSs' assignment to interrupted node i impact the IRM and highlights the endogenous uncertainty nature of the IRM r_i. The equality (2) underscores that the IRM of an interrupted node is a decreasing function of the time needed to restore power, i.e., travel and waiting times. This shows how the delayed availability of MPSs impacts the overall time to restore power at the interrupted nodes and how this deflates the number of restorative actions carried out on a timely basis. The busier the MPS assigned to an interrupted node, the less likely for this node to be immediately served, thereby increasing delays and waiting times, and leading to longer full restoration.

III. Problem Formulation

In this section, we propose a new MPS optimization model **(MPSOM)** that captures the endogenous uncertainty nature of the proposed IRM metric. The **MPSOM** model with endogenous uncertainty in waiting times and the IRM is formulated as an MINLP problem with the following objective function:

$$\max \sum_{i\in\mathbf{B}} \alpha_i (p_i^d - P_i^0) r_i - \sum_{m\in\mathbf{M}} \sum_{k\in\mathbf{K}} \sum_{i\in\mathbf{B}} C_{ik}\mu_{mki} - \sum_{m\in\mathbf{M}} \delta_m \psi_m^+ \qquad (3)$$

The objective function maximizes the total restoration benefit realized through effective management of MPSs in the DS. The first term reflects the total value of the expected restored load across the DS considering the IRM of each interrupted node i impacted by the possible non-immediate availability of MPS to service them. The difference $(p_i^d - P_i^0)$ is the amount of power restored and its multiplication by r_i is the expected power restored without delay. The second term reflects the MPSs' operation cost due to the number of trips they make and the distances traveled during the restoration process, and the third term represents the MPSs' cost for output power. The objective function (3) is nonlinear due to the endogenous uncertainty nature of r_i which requires the introduction of bilinear terms. The model has a mixed-integer nonlinear feasible set defined by the constraints described in sub-sections III-A–III-F.

We here briefly illustrate the concept of IRM through a simple example. We consider a simple network with a single-line damaged branch between nodes $n1$ and $n2$ (see Fig. 1), which results in interruption of nodes $n2$ and $n3$. Assume that the MPS station is at node $n1$ and that only one MPS is located at this station. The time needed for the MPS to reach node $n2$ from $n1$ is set to 5 minutes ($t_2 = 5$), the time needed for the MPS to reach node $n3$ from $n1$ is set to 15 minutes ($t_3 = 15$), and the time needed for the MPS to reach node $n3$ from $n2$ is 10 minutes ($t_{3'} = 10$). The value of the restored load at node $n3$ is \$5/kW ($\alpha_3 = 5$) and the final real power demand at nodes $n2$ and $n3$ following the restoration process are $p_2^d = 10$ kW and $p_3^d = 10$ kW. The restoration time horizon is assumed to be 1 hour. The simplified objective function maximizes the total restoration benefit formulated as:

$$\max \sum_{i\in\{1,2,3\}} \alpha_i (p_i^d - P_i^0) r_i$$

where i denotes the node index, and P_i^0 represents the total survived demand following an HILP event (for simplicity $P_i^0 = 0$), and r_i denotes the IRM corresponding to node i. To illustrate how the MPS travel and waiting times affect the IRM and the restoration process, we consider the following scenarios: Scenario 1 ("ideal case") where the restoration process begins immediately; as a result, the restoration benefit is equal to $5 * 10 * 1 = \$50$. Scenario 2 demonstrates the "impact of travel time", where the MPS travels from node $n1$ to $n3$ with normalized travel time $t_3 = \frac{15}{60} = 0.25$ and the corresponding value of the restoration benefit is found $5 * 10 * (1 - 0.25) = \$37.5$. Scenario 3 demonstrates the "impact of travel and waiting time", where the MPS travels from node $n1$ to $n2$ and stays there to restore the power for 15 minutes, and then it travels from node $n2$ to $n3$. The IRM at node $n3$ is equal to $r_3 = 1 - (\frac{10}{60} + \frac{20}{60}) = 0.5$ and the corresponding restoration benefit is $5*10*0.5 = \$25$. Different from the state-of-the-art models where nodal waiting times for service restoration are neglected or simply estimated ex-ante as fixed parameters, this example highlights the need to consider the waiting time in the service restoration process. This is because, in practice, MPS vehicles may not be readily available to serve the interrupted nodes immediately. This observation motivates the proposed problem formulation with endogenous uncertainty.

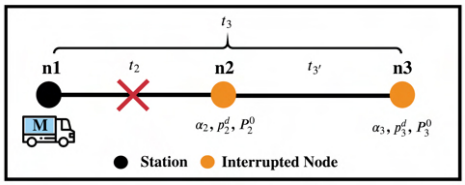

Fig. 1. The example network to demonstrate the proposed concept of IRM.

A. MPS Connection Constraints

To ease the notations, we define the index set $\mathbb{V} = \{(m, k, i) : m \in \mathbf{M}, k \in \mathbf{K}, i \in \mathbf{B}\}$. Constraint (4a) ensures that the number of nodes serviced by an MPS m located at a station k does not exceed a certain threshold M_{mk}, which represents the maximum number of trips that can be made by MPS m. Constraint (4b) ensures that each interrupted node i is assigned to at most one MPS. Constraint (4c) enforces that the number of MPSs located across all stations is equal to the number $|M|$ of units available for DS restoration. Constraint (4d) ensures that each MPS m is initially assigned to only one station k. Constraint (4e) reflects that the number of MPSs located at station k does not exceed the maximum number of spots c_k available at station k. Constraint (4f) defines the proposed IRM which can take any value between 0 and 1 due to constraint (1e). Constraints (4g) and (4h) define the integrality restrictions.

$$\sum_{i\in\mathbf{B}} \mu_{mki} \le M_{mk} y_{mk} \qquad m\in\mathbf{M}, k\in\mathbf{K} \quad (4a)$$

$$\sum_{m\in\mathbf{M}}\sum_{k\in\mathbf{K}} \mu_{mki} \le 1 \qquad i\in\mathbf{B} \quad (4b)$$

$$\sum_{k\in\mathbf{K}}\sum_{m\in\mathbf{M}} y_{mk} = |M| \quad (4c)$$

$$\sum_{k\in\mathbf{K}} y_{mk} \le 1 \qquad m\in\mathbf{M} \quad (4d)$$

$$\sum_{m\in\mathbf{M}} y_{mk} \le c_k \qquad k\in\mathbf{K} \quad (4e)$$

(1a) – (1e)

$$r_i = 1 - (t_i + w_i) \qquad i\in\mathbf{B} \quad (4f)$$

$$y_{mk} \in \{0,1\} \qquad k\in\mathbf{K}, m\in\mathbf{M} \quad (4g)$$

$$\mu_{mki} \in \{0,1\} \qquad (m,k,i)\in\mathbb{V} \quad (4h)$$

B. Power Balance Constraints

Constraints (5a) and (5b) describe the real and reactive power balance conditions at all nodes, respectively. Constraint (5c) ensures that the restored load does not exceed the maximum demand at node i. We assume that the demand power factor is fixed and calculated as $(\overline{Q}_i^d/\overline{P}_i^d)$. The relationship between the restored real and reactive load is defined by (5d). The real and reactive power flows in online branches are respectively limited by their real and reactive power capacities in (5e)-(5f). The lower and upper bounds for the real and reactive power generation at substation node (node 1) are set by constraints (5g) and (5h). Assuming no other distributed generators across the network, stationary sources of real and reactive power generation are only available at the substation node, which is enforced by constraint (5i).

$$\sum_{l(i,j)\in\mathbf{L}} p_l^f + p_i^d = \sum_{l(j,i)\in\mathbf{L}} p_l^f + p_i^g + p_i \qquad i\in\mathbf{B} \quad (5a)$$

$$\sum_{l(i,j)\in\mathbf{L}} q_l^f + q_i^d = \sum_{l(j,i)\in\mathbf{L}} q_l^f + q_i^g + q_i \qquad i\in\mathbf{B} \quad (5b)$$

$$0 \le p_i^d \le \overline{P}_i^d \qquad i\in\mathbf{B} \quad (5c)$$

$$q_i^d = p_i^d(\overline{Q}_i^d/\overline{P}_i^d) \qquad i\in\mathbf{B} \quad (5d)$$

$$-\lambda_l\overline{P}_l \le p_l^f \le \lambda_l\overline{P}_l \qquad l\in\mathbf{L} \quad (5e)$$

$$-\lambda_l\overline{Q}_l \le q_l^f \le \lambda_l\overline{Q}_l \qquad l\in\mathbf{L} \quad (5f)$$

$$\underline{P}^g \le p_1^g \le \overline{P}^g \quad (5g)$$

$$\underline{Q}^g \le q_1^g \le \overline{Q}^g \quad (5h)$$

$$p_i^g = q_i^g = 0 \qquad i\in\mathbf{B}\setminus\{1\} \quad (5i)$$

C. Power Flow Constraints

Constraints (6a) and (6b) represent the power flow equation considering the status of branches where the term $(1-\lambda_l)M^v$ or $(\lambda_l - 1)M^v$ ensures that the power flow condition is satisfied for connected branches [31]. The parameter M^v is the maximum value for the difference in the squared voltage magnitudes between nodes i and j connected by branch l. If the branch l between nodes i and j is connected ($\lambda_l = 1$), then the terms $(1-\lambda_l)M^v$ and $(\lambda_l - 1)M^v$ vanish from (6a) and (6b). If the branch is disconnected ($\lambda_l = 0$), the second term will be 0—see (5e) and (5f). Constraint (6c) states the limits for the squared voltage magnitudes at any node i.

$$V_i^s - V_j^s \le (1-\lambda_l)M^v + 2(R_l p_l^f + X_l q_l^f) \quad i,j\in\mathbf{B}, l\in\mathbf{L} \quad (6a)$$

$$V_i^s - V_j^s \ge (\lambda_l - 1)M^v + 2(R_l p_l^f + X_l q_l^f) \quad i,j\in\mathbf{B}, l\in\mathbf{L} \quad (6b)$$

$$\underline{V}_i^s \le V_i^s \le \overline{V}_i^s \qquad i\in\mathbf{B} \quad (6c)$$

D. MPS Output Power Constraints

The total real and reactive power supplied by MPSs at node i is equal to the sum of the real and reactive power output of each MPS assigned to node i—see constraints (7a) and (7b). Constraints (7c) and (7d) guarantee that the real and reactive power output of MPS m do not exceed the respective limits.

$$p_i = \sum_{m\in\mathbf{M}}\sum_{k\in\mathbf{K}} \psi_m^+ \mu_{mki} \qquad i\in\mathbf{B} \quad (7a)$$

$$q_i = \sum_{m\in\mathbf{M}}\sum_{k\in\mathbf{K}} \psi_m^- \mu_{mki} \qquad i\in\mathbf{B} \quad (7b)$$

$$0 \le \psi_m^+ \le \Psi_m^+ \qquad m\in\mathbf{M} \quad (7c)$$

$$0 \le \psi_m^- \le \Psi_m^- \qquad m\in\mathbf{M} \quad (7d)$$

E. Branch Status Constraints

DS reconfiguration is one common practice for service restoration following an HILP incident. DS reconfiguration is achieved through the operation of remotely-controlled switches (RCSs) across the network [32]. The DS operator can control the ON/OFF status of the RCSs to change the network connectivity. The binary variable λ_l indicates whether branch l is connected ($\lambda_l = 1$) or not ($\lambda_l = 0$). The status of the branches equipped with RCSs can be changed during the restoration process. However, DS reconfiguration does not apply to damaged branches as enforced in constraint (8a). Constraint (8b) indicates that undamaged branches without RCSs are always kept connected during the restoration process.

$$\lambda_l = 0 \qquad l\in\mathbf{L^d} \quad (8a)$$

$$\lambda_l = 1 \qquad l\in\mathbf{L}\setminus\{\mathbf{L^d},\mathbf{L^s}\} \quad (8b)$$

$$\lambda_l \in \{0,1\} \qquad l\in\mathbf{L} \quad (8c)$$

F. DS Radiality Constraints

Radiality constraints (9a)-(9e) are introduced to maintain the radial topology of the DS [1]. There are two significant reasons for the DS to be operated with a radial topology [33]: (i) to facilitate the network protection coordination; (ii) to reduce the short-circuit current in the DS. While DSs can have a meshed (i.e., loop) structure, they are normally operated as radial for effective coordination of their protection systems under emergency and faulted operating conditions [34]. Branch damages due to an HILP event result in several physical islands (PIs) in which all load nodes are disconnected from the main grid. The relationship between the number of available branches and the number of PIs is presented in the electronic Appendix [35]. Constraint (9a) states that the number of connected branches is equal to the number of nodes in DS minus the number of PIs caused by damaged branches [1], [5]. Each PI is modeled via fictitious supply and demand nodes. In each PI, one node is considered to be a fictitious supply node and the remaining nodes are fictitious load nodes. The concept of fictitious flow also needs to be introduced to establish the connection between fictitious supply and load

nodes in a PI. Constraints (9b) and (9c) ensure the fictitious flow balance for the fictitious supply and load nodes—similar to (5a) and (5b). Here, the fictitious load d_i^f is set to be 1 at all load nodes. Constraint (9d) stipulates the direction and the amount of fictitious power flow. Constraint (9d) enforces that the fictitious supply at node i cannot exceed its maximum limit M^s.

$$\sum_{l\in\mathbf{L}} \lambda_l = N - N^i \tag{9a}$$

$$\sum_{l(i,j)\in\mathbf{L}} f_l - \sum_{l(j,i)\in\mathbf{L}} f_l = f_i^g \qquad i\in\mathbf{B^s} \tag{9b}$$

$$\sum_{l(j,i)\in\mathbf{L}} f_l - \sum_{l(i,j)\in\mathbf{L}} f_l = d_i^f \qquad i\in\mathbf{B}\setminus\mathbf{B^s} \tag{9c}$$

$$-\lambda_l M^f \le f_l \le \lambda_l M^f \qquad l\in\mathbf{L} \tag{9d}$$

$$0 \le f_i^g \le M^s \qquad i\in\mathbf{B^s} \tag{9e}$$

IV. Solution Method

We here examine the properties and tractability of the MINLP problem **MPSOM**. We first note that the continuous relaxation of problem **MPSOM**

$$\begin{aligned}\max\ & \sum_{i\in\mathbf{B}} \alpha_i(p_i^d - P_i^0)r_i - \sum_{m\in\mathbf{M}} \delta_m\psi_m^+ \\ & - \sum_{m\in\mathbf{M}}\sum_{k\in\mathbf{K}}\sum_{i\in\mathbf{B}} C_{ik}\mu_{mki} \\ \text{s.to}\ & (1a)-(1e),(4a)-(9e)\end{aligned} \tag{10}$$

is nonconvex. Indeed, problem **MPSOM** has nonlinear equality constraints (1c), (7a), and (7b), which implies that the feasible area is not convex and that **MPSOM** is not a convex problem regardless of the integrality restrictions on some decision variables.

We shall now derive an MILP reformulation for problem **MPSOM** by using several linearization methods for small-degree polynomial terms. The sources of nonconvexity in **MPSOM** are due to the bilinear terms: 1) $r_i p_i^d$ with products of continuous variables, 2) $\psi_m^+\mu_{mki}$ and $\psi_m^-\mu_{mki}$ with products of a binary by a continuous variable. Note that the McCormick inequalities [36] applied to the product of two continuous variables can only provide a linear relaxation and the convex envelope of bilinear terms. The properties of our model allow us to exactly reformulate products of two continuous variables and is a key contribution. The following two lemmas will be used in the proof of Theorem 1.

Lemma 1: [36] Let $x\in\{0,1\}$ and $y\in[0,\bar{y}]\subset\mathbb{R}^+$. The bilinear term xy can be linearized by the set $\mathcal{M}_{xy}^z := \{(x,y,z)\in\{0,1\}\times[0,\bar{y}]^2 : (11a)-(11d)\}$ of linear inequalities

$$\mathcal{M}_{xy}^z := \begin{cases} z\ge 0 & (11a)\\ z\ge y + x\bar{y} - \bar{y} & (11b)\\ z\le y & (11c)\\ z\le \bar{y}x & (11d)\end{cases}$$

that ensures that $z := xy$.

Lemma 2: Lemma 2 is a direct extension of lemma 1 for a trilinear term of that form. Let $x=[x_1,x_2]\in\{0,1\}^2$ and $y\in[0,\bar{y}]\subset\mathbb{R}^+$. The trilinear term x_1x_2y can be linearized by the set $\mathcal{M}_{x_1x_2y}^w := \{(x_1,x_2,y,w)\in\{0,1\}^2\times[0,\bar{y}]^2 : (12a)-(12e)\}$ of linear inequalities

$$\mathcal{M}_{x_1x_2y}^w := \begin{cases} w\ge 0 & (12a)\\ w\ge \bar{y}(x_1+x_2-2)+y & (12b)\\ w\le y & (12c)\\ w\le \bar{y}x_1 & (12d)\\ w\le \bar{y}x_2 & (12e)\end{cases}$$

that ensures that $w := x_1x_2y$.

Theorem 1 shows how we can linearize such bilinear terms by exploiting the structure of the problem. We define the index set $\mathbb{W} = \{(m,k,i,i') : m\in\mathbf{M}, k\in\mathbf{K}, i,i'\in\mathbf{B} : i>1, i'i\}$.

Theorem 1: Let $\theta,\zeta,\beta,\kappa,\gamma,\eta$ be vectors of the nonnegative auxiliary decision variables. Problem **R-MPSOM**:

$$\begin{aligned}\max\ & \sum_{i\in\mathbf{B}} \alpha_i(p_i^d - \kappa_i - \eta_i - P_i^0 r_i) - \sum_{m\in\mathbf{M}} \delta_m\psi_m^+ \\ & - \sum_{m\in\mathbf{M}}\sum_{k\in\mathbf{K}}\sum_{i\in\mathbf{B}} C_{ik}\mu_{mki} \qquad (13a)\\ \text{s.to}\ & (1e),(4a)-(4e),(4g)-(6c),(8a)-(9e)\end{aligned}$$

$$p_i = \sum_{m\in\mathbf{M}}\sum_{k\in\mathbf{K}} \theta_{mki}, \qquad i\in\mathbf{B} \tag{13b}$$

$$q_i = \sum_{m\in\mathbf{M}}\sum_{k\in\mathbf{K}} \zeta_{mki}, \qquad i\in\mathbf{B} \tag{13c}$$

$$\theta_{mki} \ge 0 \qquad (m,k,i)\in\mathbb{V} \tag{13d}$$

$$\theta_{mki} \ge \Psi_m^+(\mu_{mki}-1) + \psi_m^+ \qquad (m,k,i)\in\mathbb{V} \tag{13e}$$

$$\theta_{mki} \le \psi_m^+ \qquad (m,k,i)\in\mathbb{V} \tag{13f}$$

$$\theta_{mki} \le \Psi_m^+\mu_{mki} \qquad (m,k,i)\in\mathbb{V} \tag{13g}$$

$$\zeta_{mki} \ge 0 \qquad (m,k,i)\in\mathbb{V} \tag{13h}$$

$$\zeta_{mki} \ge \Psi_m^-(\mu_{mki}-1) + \psi_m^- \qquad (m,k,i)\in\mathbb{V} \tag{13i}$$

$$\zeta_{mki} \le \psi_m^- \qquad (m,k,i)\in\mathbb{V} \tag{13j}$$

$$\zeta_{mki} \le \Psi_m^-\mu_{mki} \qquad (m,k,i)\in\mathbb{V} \tag{13k}$$

$$\kappa_i = \sum_{k\in\mathbf{K}}\sum_{m\in\mathbf{M}} T_{ik}\beta_{mki} \qquad i\in\mathbf{B} \tag{13l}$$

$$\beta_{mki} \ge 0, \qquad (m,k,i)\in\mathbb{V} \tag{13m}$$

$$\beta_{mki} \ge p_i^d + \overline{P}_i^d(\mu_{mki}-1) \qquad (m,k,i)\in\mathbb{V} \tag{13n}$$

$$\beta_{mki} \le \overline{P}_i^d\mu_{mki} \qquad (m,k,i)\in\mathbb{V} \tag{13o}$$

$$\beta_{mki} \le p_i^d \qquad (m,k,i)\in\mathbb{V} \tag{13p}$$

$$\eta_i = \sum_{m\in M}\sum_{k\in K}\sum_{i'=1}^{i-1}(T_{i'k}+\tau_{mi'})\gamma_{mkii'} \qquad i\in\mathbf{B} \tag{13q}$$

$$\eta_1 = 0 \tag{13r}$$

$$\gamma_{mkii'} \ge 0 \qquad (m,k,i,i')\in\mathbb{W} \tag{13s}$$

$$\gamma_{mkii'} \ge \overline{P}_i^d(\mu_{mki}+\mu_{mki'}-2) + p_i^d \ (m,k,i,i')\in\mathbb{W} \tag{13t}$$

$$\gamma_{mkii'} \le \mu_{mki}\overline{P}_i^d \qquad (m,k,i,i')\in\mathbb{W} \tag{13u}$$

$$\gamma_{mkii'} \le p_i^d \qquad (m,k,i,i')\in\mathbb{W} \tag{13v}$$

is equivalent to problem **MPSOM** and has a convex continuous reformulation.

Proof. *(i)* We first reformulate the nonlinear constraints (7a) and (7b), and use Lemma 1 to linearize the bilinear terms $\psi_m^+\mu_{mki}$ and $\psi_m^-\mu_{mki}$. Let Ψ_m^+ and Ψ_m^- denote the upper bounds of the nonnegative variables ψ_m^+ and ψ_m^-. The linearization of (7a) and (7b) is accomplished by introducing the McCormick inequalities (13d)-(13g) for each term $\psi_m^+\mu_{mki}$ and another one (13h)-(13k) for each $\psi_m^-\mu_{mki}$, which ensures that; $\theta_{mki} := \psi_m^+\mu_{mki}$ and $\zeta_{mki} := \psi_m^-\mu_{mki}$. Constraints (13b) and (13c) enforce that each term p_i and q_i is respectively equal to the sum of the variables θ_{mki} and ζ_{mki} representing the bilinear terms in (7a) and (7b).
(ii) We now reformulate and linearize the products $r_i p_i^d$ of continuous variables in the objective function. Using (4f), we can rewrite the objective function (13a) in a lifted space as:

$$\sum_{i\in\mathbf{B}} \alpha_i(p_i^d - P_i^0)r_i = \sum_{i\in\mathbf{B}} \alpha_i p_i^d\Big(1-(t_i+w_i)\Big) - \sum_{i\in\mathbf{B}} \alpha_i P_i^0 r_i$$
$$= \sum_{i\in\mathbf{B}} \alpha_i\Big(p_i^d - (p_i^d t_i + p_i^d w_i)\Big) - \sum_{i\in\mathbf{B}} \alpha_i P_i^0 r_i \quad (14)$$

Two sets of bilinear terms — $p_i^d t_i$ and $p_i^d w_i$ — appear now.
(ii.1) We start with the linearization of the products $p_i^d t_i$ of continuous variables, which, using (1a), can be rewritten as:

$$p_i^d t_i = \sum_{k\in\mathbf{K}}\sum_{m\in\mathbf{M}} T_{ik}\mu_{mki}p_i^d \qquad i\in\mathbf{B} \qquad (15)$$

Each equality (15) reformulates the corresponding bilinear term $p_i^d t_i$ as a sum of bilinear terms with weighted (by parameters T_{ik}) products of a binary μ_{mki} by a continuous variable p_i^d upper-bounded by $\overline{P}_i^d$. Using Lemma 1, the bilinear terms $p_i^d t_i$ can be exactly reformulated and linearized with the McCormick inequalities (13m)-(13p) which forces $\beta_{mki} := \mu_{mki}p_i^d$. The linear constraint (13l) ensures that the new variable κ_i is equal to the weighted sum of the new variables β_{mki} introduced in the linearization process.
(ii.2) In order to linearize the terms $p_i^d w_i$, we use (1c) and (1d) to rewrite them

$$p_i^d w_i = p_i^d \sum_{m\in M}\sum_{k\in K}\left(\mu_{mki}\left(\sum_{i'=1}^{i-1}\mu_{mki'}(T_{i'k}+\tau_{mi'})\right)\right) \quad (16)$$

as sums of trilinear terms $p_i^d\mu_{mki}\mu_{mki'}$ with products of two binary variables by a continuous one. Introducing the vector of non-negative continuous variables γ and applying Lemma 2, we linearize these trilinear terms with the set of linear inequalities (13s)-(13v) which guarantee $\gamma_{mkii'} := p_i^d\mu_{mki}\mu_{mki'}, (m,k,i,i') \in \mathbb{W}$. The linear constraint (13q) ensures that the new variable η_i is equal to the weighted sum of the new variables γ_{mki} introduced in the linearization process. All polynomial terms in the objective function and constraints of the problem **MPSOM** are exactly reformulated with linear inequalities, which provides the result we set out to prove. □

V. Numerical Results and Discussions

In this section, the proposed model and solution approach are applied to the IEEE 33-node and IEEE 123-node test systems. The IEEE 33-node test system includes 1 substation, 32 branches, 33 nodes, and 5 normally open RCSs [31] — see Fig. 2. The IEEE 123-node test system owns 1 substation, 122 branches, 123 nodes, and 5 normally open RCSs [37] — see Fig. 3. Note that the proposed **MPSOM** framework is a deterministic model designed in response to one forecasted damage scenario in the network. In order to verify the effectiveness of the presented scheme for DS restoration and in capturing the endogenous uncertainties in MPSs availability, we study a series of single- and multi-line damage scenarios in each test system, as a result of which full (worst-case) or partial electricity outages may be realized. We run the proposed **MPSOM** model for each forecasted damage scenario where the optimal decisions on the MPSs pre-positioning (before the event), as well as their routing and dispatch (following the event) are made concurrently. The proposed model is aimed at enhanced resilience delivery in the electric power DS and is generic enough to accommodate any additional constraints and considerations of the transportation system. The tests are conducted on a PC with an Intel Xeon E5-2620 v2 processor and 16 GB memory. The optimization problems are formulated with AMPL and solved with the state-of-the-art optimization solvers Baron 19.12.7 for the MINLP problem **MPSOM** and Gurobi 9.0.2 for the MILP problem **R-MPSOM**.

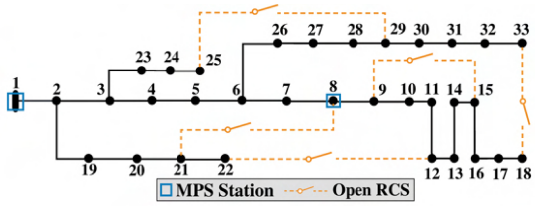

Fig. 2. The studied IEEE 33-node test system with MPS stations.

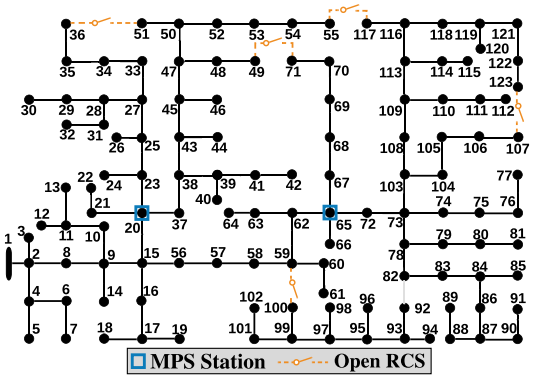

Fig. 3. The studied IEEE 123-node test system with MPS stations.

A. MPSs Routing and Scheduling Assignments

We illustrate here the detailed MPSs routing and scheduling assignments with the corresponding IRM values obtained with the proposed model and its application to the IEEE 33-node and IEEE 123-node test systems. The greater the value of the IRM, the faster the interrupted node is restored by MPSs (where $IRM = 1$ is indicative of an immediate service restoration). In order to verify the efficiency of proposed model for DS restoration, the maximum admissible time for system restoration is set to 1 hour for both systems.

1) IEEE 33-Node Test Systems: The IEEE 33-node test system is assumed to be equipped with 2 MPS stations located at nodes $n1$ and $n8$ (see Figure 2), and 3 MPSs with 800 KW/600 kVar capacity can be hosted in any of these stations. Figure 4 illustrates the MPSs assignments under two multi-line damage scenarios in the IEEE 33-node test system with the corresponding IRM values.

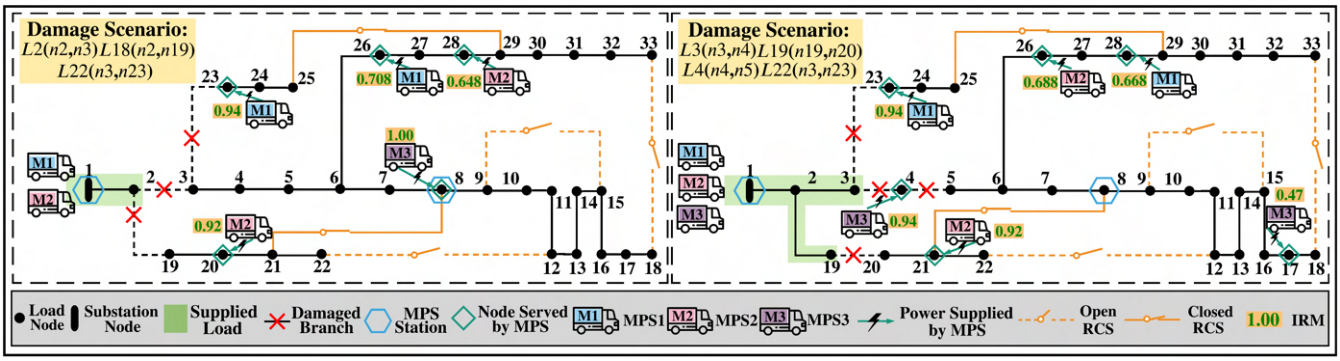

Fig. 4. MPSs assignments for response and recovery in the face of extreme events: IEEE 33-node test system.

In the three-line damage scenario with damaged branches $L2$, $L18$, and $L22$, 2 RCSs are closed to help in DS restoration: the RCS between nodes $n8$ and $n21$, and the RCS between nodes $n25$ and $n29$. Both MPS1 and MPS2 are assigned from station 1. MPS1 provides power to $n23$ with an IRM equal to 0.94, and then moves to $n26$ with an IRM of 0.708. MPS2 is sent to $n21$ and $n26$ with the IRM values of 0.92 and 0.648, respectively. Located at station 2, MPS3 supplies $n8$ immediately. In this scenario, it takes nearly 21 minutes for the MPSs to reach the designated nodes during the restoration process, resulting in full-service recovery within 1 hour. In Figure 4, all 3 MPSs are assigned from station 1 in the four-line damage scenario with damaged branches $L3$, $L4$, $L19$, and $L22$. MPS1 is sent to $n24$ with an IRM value of 0.94, then to $n28$ with an IRM value of 0.668. Node $n21$ is supplied by MPS2 with an IRM value of 0.92, and then moves to $n26$ with an IRM value of 0.688. MPS3 is assigned to $n4$ with an IRM value of 0.94, and then to $n17$ with around 32 minutes delay (IRM equals 0.47). Furthermore, the same two normally open RCSs as in the three-line damage scenario mentioned above are closed to participate in DS restoration.

2) IEEE 123-Node Test System: The IEEE 123-node test system is assumed to be equipped with 2 MPS stations located at nodes $n20$ and $n65$ (see Figure 3), each of which capable of hosting 3 MPSs with 800kW/600 kVar capacity. Figure 5 illustrates the MPSs assignments in three multi-line damage scenarios in the IEEE 123-node test system with the corresponding IRM values.

For the multi-line damage scenario, where branches $L8$, $L10$, and $L17$ are damaged, all MPSs are positioned and deployed from station 1. MPS1 immediately serves node $n20$ and then travels to restore node $n92$ with an IRM value of 0.72. MPS2 first serves node $n28$ with an IRM value of 0.94 and then travels to node $n83$ with an IRM value of 0.72. Lastly, MPS3 serves node $n11$ with an IRM value of 0.95. Meanwhile, the normally-open RCS between $n49$ and $n71$ are closed to facilitate the DS service restoration. Similarly, in another damage scenario where branches $L8$, $L10$, $L62$ and $L63$ are damaged, all 3 MPSs are assigned to participate in the restoration process. The results show that MPS1 (located at station 2) immediately begins the restoration process at node $n65$ and then travels to restore $n92$ with an IRM value of 0.799. MPS2 (located and station 2) first serves node $n59$ with an IRM value of 0.985 and reaches node $n83$ with a 13-minute delay (IRM equal to 0.789). Located at station 1, MPS3 serves $n9$ with the IRM value of 0.973. Note that the normally-open RCS between $n49$ and $n71$, and also between $n55$ and $n117$ are closed to facilitate the DS restoration.

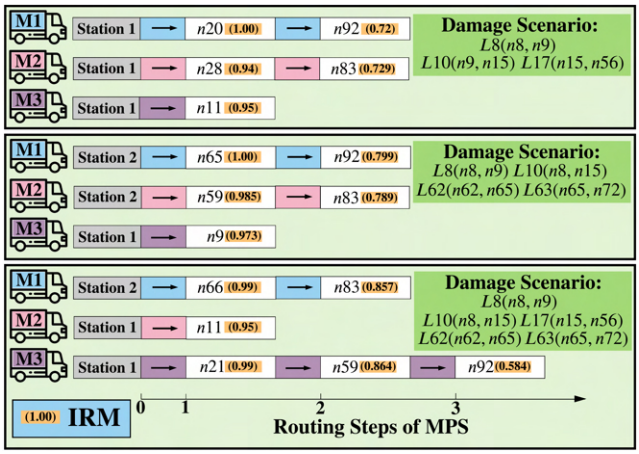

Fig. 5. MPSs assignments for restoration: IEEE 123-node test system.

B. Computational Efficiency

We now compare the computational efficiency of the MINLP model **MPSOM** solved with the Baron solver and of the MILP model **R-MPSOM** solved with the Gurobi solver. The tolerance level for each solver is set to 0.01%. To carry out this analysis, we generate 4 single-line and 6 multi-line damage scenarios for each test system. Table I and Table II report the computational time for the two models under single-line and multi-line damage scenarios, respectively.

For all single-line damage scenarios in the IEEE 33-node test system, one can observe from Table I that (i) the MINLP model **MPSOM** is solved to optimality (tolerance level $\leq 0.01\%$) within 1 hour, and (ii) the optimal solutions for the MILP model **R-MPSOM** are obtained much faster than those for the MINLP model **MPSOM**. In particular, Table I shows that the MILP problem's solution time for scenario S1 (resp., S2, S3, and S4) for the IEEE 33-node test system is of 2.51 seconds (resp., 1.72, 1.19, and 1.22) while, for the MINLP problem, it amounts to 39.33 seconds (resp., 38.2, 19.55, and 14.45). This indicates that the MILP problem can be solved 15.6 (resp., 22.2, 16.5, and 11.8) times quicker than the MINLP problem for scenario S1 (resp., S2, S3, and S4). Focusing on the IEEE 123-node test system, the results presented in Table I show that the MINLP model could not be always solved to optimality within 1 hour (e.g., S1 and S2 with respective optimality gaps of 0.11% and

0.12%). However, the suggested MILP model **R-MPSOM** could always be solved to optimality very quickly. These observations once again attest to the increased difficulty of solving a nonconvex MINLP problem and the benefits of the developed linearization procedure.

Similar observations prevail for the multi-line damage scenarios whose results are given in Table II. The MILP model **R-MPSOM** is solved to optimality very quickly for each scenario. However, the MINLP formulation could only be solved in one hour for seven of the twelve tested scenarios (i.e., six of those correspond to the IEEE 33-node test system and one to the IEEE 123-node test system). The solution time of the MILP model is, on average, around 45 times smaller than that of the MINLP model (4.18 sec. vs. 190.06 sec.).

The analyses over all outage scenarios in both test systems (see Table I and Table II) demonstrate that, despite having a (much) larger number of decision variables and linear constraints, the linearity feature – and the resulting convexity of the continuous relaxation – makes it significantly faster to find the optimal solution and to prove its optimality with the proposed MILP model. The scalability of the MILP model makes it employable for larger and more complex instances.

TABLE I
COMPUTATIONAL PERFORMANCE COMPARISONS UNDER SINGLE-LINE DAMAGE SCENARIOS

IEEE 33-Node Test System			
Scenarios	**Damaged**	**Computation Time (sec.)**	
(S)	**Line**	**MILP**	**MINLP**
S1	$L1$	2.515	39.328
S2	$L2$	1.719	38.188
S3	$L3$	1.188	19.547
S4	$L4$	1.224	14.453
IEEE 123-Node Test System			
Scenarios	**Damaged**	**Computation Time (sec.)**	
(S)	**Line**	**MILP**	**MINLP**
S1	$L1$	1442.56	3600 (0.11%*)
S2	$L2$	1631.933	3600 (0.12%*)
S3	$L8$	1712.688	3600 (0.15%*)
S4	$L10$	1952.921	3600 (0.16%*)

*Optimality gap for MINLP model after one hour

TABLE II
COMPUTATIONAL PERFORMANCE COMPARISONS IN MULTI-LINE DAMAGE SCENARIOS

IEEE 33-Node Test System			
Scenarios	**Damaged**	**Computation Time (sec.)**	
(S)	**Lines**	**MILP**	**MINLP**
S1	$L2$-$L18$-$L22$	2.828	45.109
S2	$L5$-$L6$-$L25$	1.578	31.375
S3	$L3$-$L4$-$L19$-$L22$	4.906	78.984
S4	$L5$-$L24$-$L25$-$L26$	4.297	224.203
S5	$L2$-$L3$-$L19$-$L22$-$L23$	9.032	683.25
S6	$L5$-$L6$-$L7$-$L24$-$L25$	2.453	77.438
IEEE 123-Node Test System			
Scenarios	**Damaged**	**Computation Time (sec.)**	
(S)	**Lines**	**MILP**	**MINLP**
S1	$L8$-$L10$-$L17$	538.594	3600 (0.044%*)
S2	$L17$-$L21$-$L23$	100.188	1548.58
S3	$L8$-$L10$-$L62$-$L63$	1083.58	3600 (0.053%*)
S4	$L21$-$L23$-$L70$-$L71$	244.406	3600 (0.061%*)
S5	$L8$-$L10$-$L17$-$L62$-$L63$	1575.75	3600 (0.091%*)
S6	$L10$-$L16$-$L17$-$L62$-$L63$	1430.86	3600 (0.059%*)

*Optimality gap for MINLP model after one hour

C. Modeling Endogenous Uncertainty in the Waiting Time for Restoration: Quantification of Benefits

To further evaluate the IRM metric in DS restoration, we here compare the proposed **R-MPSOM** formulation (with waiting times modeled as endogenous uncertainties) with traditional approaches in which either only travel times are considered and waiting times are ignored (Case 1) or busy probabilities and waiting times are estimated as a fixed parameter set prior to solving the optimization model (Case 2).

The mathematical formulation for Case 1 model – which ignores waiting times – reads as follows:

$$\max \sum_{i\in\mathbf{B}} \alpha_i(p_i^d - \kappa_i - P_i^0 r_i) - \sum_{m\in\mathbf{M}} \delta_m \psi_m^+ - \sum_{m\in\mathbf{M}}\sum_{k\in\mathbf{K}}\sum_{i\in\mathbf{B}} C_{ik}\mu_{mki} \tag{17a}$$

$$\text{s.to } (4a)-(4e),(4g)-(6c),(8a)-(9e),(13b)-(13p)$$

$$t_i \le 1 \qquad i\in\mathbf{B} \tag{17b}$$

$$r_i = 1 - t_i \qquad i\in\mathbf{B} \tag{17c}$$

Note that constraints (17b) and (17c) are analogous to (1e) and (4f) since the waiting times are ignored: $v_{mki} = w_i = 0, i\in\mathbf{B}, k\in\mathbf{K}, m\in\mathbf{M}$.

To obtain the mathematical formulation for Case 2, we assume that the busy probability of each MPS, and therefore the waiting times associated with each MPS assignment, is known and computed ex-ante. The assumed MPSs' busy probability is denoted as π_m and can be estimated as the ratio of the average number of requests per hour to the product of the number of MPSs that are deployed by the average service time per request [38]. This approximation ex-ante of the (assumed) busy probability, also called normalized workload, is commonly used in the literature (see, e.g., [38]). We accordingly update the objective function as:

$$\sum_{i\in\mathbf{B}} \alpha_i(p_i^d - P_i^0)\Big(1 - \Big(\sum_{k\in\mathbf{K}}\sum_{m\in\mathbf{M}} \mu_{mki}(T_{ik}+\pi_m)\Big)\Big) \tag{18}$$

As a result, the model **R-MPSOM-W** corresponding to Case 2 in which the busy probability is the same for each MPS and is a fixed parameter estimated ex-ante reads:

$$\max \sum_{i\in\mathbf{B}} \alpha_i(p_i^d - \nu_i) - \sum_{m\in\mathbf{M}}\sum_{k\in\mathbf{K}}\sum_{i\in\mathbf{B}} C_{ik}\mu_{mki} - \sum_{i\in\mathbf{B}} \alpha_i P_i^0\Big(1 - \sum_{k\in\mathbf{K}}\sum_{m\in\mathbf{M}} \mu_{mki}(T_{ik}+\pi_m)\Big) - \sum_{m\in\mathbf{M}} \delta_m\psi_m^+ \tag{19a}$$

$$\text{s.to } (4a)-(4e),(4g)-(6c),(8a)-(9e),(13b)-(13k),(13m)-(13p)$$

$$\nu_i = \sum_{k\in\mathbf{K}}\sum_{m\in\mathbf{M}} (T_{ik}+\pi_m)\beta_{mki} \qquad i\in\mathbf{B} \tag{19b}$$

$$\sum_{k\in\mathbf{K}}\sum_{m\in\mathbf{M}} \mu_{mki}(T_{ik}+\pi_m) \le 1 \qquad i\in\mathbf{B} \tag{19c}$$

Note that the sum of bilinear terms $\mu_{mki}p_i^d$ weighted by the parameters $(T_{ik}+\pi_m)$ can be exactly reformulated and linearized with the McCormick inequalities (13m)-(13p) which forces $\beta_{mki} := \mu_{mki}p_i^d$. The linear constraint (19b) ensures that the new variable ν_i is equal to the weighted sum of

the variables β_{mki} introduced in the linearization process. Constraint (19c) guarantees that the MPSs' service time to restore node i could not exceed the maximum admissible time for system restoration (i.e., ≤ 1).

We postulate that there is value to be gained if the endogenous uncertainty in the waiting time is accounted for. We aim to demonstrate that the traditional approaches (Case I and Case II) may lead to an inaccurate estimation of the restoration benefits primarily due to their simplifying assumptions on the availability of the MPSs. We calculate the added value (additional restoration benefit) obtained by endogenizing the uncertainty in MPSs' availability and waiting times. To do so, we compare the proposed **R-MPSOM** model that accounts for endogenous uncertainty with the **R-MPSOM-T** and **R-MPSOM-W** models. In the following, we formalize the approach taken to check the validity of the assumptions underlying models **R-MPSOM-T** and **R-MPSOM-W** and to quantify the value of properly modeling the endogenous uncertainty in the availability of MPSs and in the resulting waiting time for power restoration:

1) Solve model **R-MPSOM**. Let Z^* be its optimal value and ($\mathbf{x}^*$, μ^*) be its optimal solution. The vector $\mathbf{x}$ is the concatenation of all (except μ) decision variables.
2) Solve:
   - Model **R-MPSOM-T** with no waiting times. Let ($\mathbf{x^T}^*$, μ^{T*}) denote the optimal solution.
   - Model **R-MPSOM-W** with fixed MPSs' availability and waiting times computed ex-ante. Let ($\mathbf{x^W}^*$, μ^{W*}) be the optimal solution.
3) Set (fix) μ_{mki} equal to:
   - μ^{T*}_{mki}. Calculate the resulting optimal value obtained by using the optimal solution of **R-MPSOM-T** in **R-MPSOM**. Denote the resulting value of the objective function by Z^{T*}.
   - μ^{W*}_{mki}. Calculate the resulting optimal value obtained by using the optimal solution of **R-MPSOM-W** in **R-MPSOM**. Denote the resulting value of the objective function by Z^{W*}.
4) Calculate the value of accounting for endogenous uncertainty in waiting times versus assuming that:
   - MPSs are immediately available (no waiting times): Z^*-Z^{T*}.
   - There is no uncertainty in MPSs' availability: Z^*-Z^{W*}.

TABLE III
ACTUAL MPSS' AVAILABILITY WITH MODELS **R-MPSOM-T** AND **R-MPSOM-W**: IEEE 123-NODE TEST SYSTEM

		Actual MPSs' Availability		
		MPS1	MPS2	MPS3
Damaged Lines	**R-MPSOM-T**	0.7625	0.651	0.6745
$L8$-$L10$-$L17$	**R-MPSOM-W**	0.8875	0.6225	0.666
Damaged Lines	**R-MPSOM-T**	0.655	0.7365	0.7625
$L8$-$L10$-$L62$-$L63$	**R-MPSOM-W**	0.8615	0.8875	0.509
Damaged Lines	**R-MPSOM-T**	0.7625	0.6595	0.7365
$L8$-$L10$-$L17$-$L62$-$L63$	**R-MPSOM-W**	0.526	0.8615	0.8875

We first investigate whether the *assumed* MPSs' availability is the same as (or close to) the *actual* MPSs' availability corresponding to the optimal solutions of models **R-MPSOM-T** and **R-MPSOM-W**. The actual availability of an MPS depends on its workload, i.e., the time needed to serve the interrupted nodes to which it has been assigned. The actual availability of MPS m, called the availability probability, is denoted by ρ_m and calculated as:

$$\rho_m = 1 - \sum_{i \in \mathbf{B} \setminus \{1\}} \sum_{k \in \mathbf{K}} \mu^*_{mki}(T_{ik} + \tau_{mi}) \qquad m \in \mathbf{M} \qquad (20)$$

We can compare the assumed and actual availability of MPSs. Table III provides the results for different damage scenarios in the IEEE 123-node test system. Note that the same three scenarios are represented in Figure 5.

Table III shows the fallacy of the underlying assumptions for models **R-MPSOM-T** and **R-MPSOM-W**:

- **R-MPSOM-T** model assumes that each MPS is always available to serve the interrupted nodes (i.e., the assumed MPSs' availability is set to one). The issue with this strategy can be seen by comparing the assumed vs. actual MPSs' availability (ρ_m) values. For all test scenarios, the actual MPSs' availability vary between 0.651 and 0.7625 which violates the assumption of immediate MPSs' availability. This indicates that waiting times should be taken into account and that **R-MPSOM-T** model – that ignores them – is not to be trusted.
- **R-MPSOM-W** model assumes that the MPSs' busy probabilities, and therefore the waiting times associated with each MPS assignment, are all equal, known ex-ante, and set to a fixed value. The assumed MPS' availability is $1 - \pi_m$ with π_m calculated as explained above. This gives the following assumed MPSs' availability for each scenario: 0.85 for $L8$-$L10$-$L17$ damaged lines scenario, 0.83 for $L8$-$L10$-$L62$-$L63$ damaged lines scenario, and 0.8 for $L8$-$L10$-$L17$-$L62$-$L63$ damaged lines scenario. We observe first from Table III that the actual availability differs for each MPS in all test scenarios. This observation violates the model's assumption that each MPS has the same availability (i.e., same busy probability). Additionally, the actual availability of the MPSs differs from the assumed availability. The actual availability is almost always lower than the assumed one. For example, the assumed MPSs' availability for the $L8$-$L10$-$L17$ damaged lines scenario is fixed to 0.85, while the actual availability of the three MPSs is: 0.8875, 0.6225, and 0.666. This illustrates the discrepancy between the assumed and actual availability of MPSs associated with the optimal solution of model **R-MPSOM-W**. This points out that model **R-MPSOM-W** is not suitable and challenges the validity of its underlying assumptions. More precisely, this indicates that the MPSs' availability and waiting times cannot be assumed known prior to solving the optimization model.

Table IV and V report and compare the values of Z^*, Z^{T*}, and Z^{W*} obtained for several single-line and multi-line damage scenarios in the IEEE 33-node and 123-node test systems. For each tested scenario, differences of $(Z^* - Z^{T*})$ and $(Z^* - Z^{W*})$ are always strictly positive, which confirms the need to account for the endogenous uncertainty in the IRM

metric. The obtained results show that the busy probability of each MPS, and therefore the waiting times associated with each MPS assignment, should not be modeled as a fixed parameter due to the loss in the total restoration benefit. Contrary to the model with an estimated busy probability and waiting times that requires re-estimations for each damaged-line scenario, modeling waiting time as an endogenous source of uncertainty allows for levels of adaptivity to any delays and MPS travel settings that might be realized during the real-world HILP incidents. The endogenization of the waiting time as an endogenous uncertainty can be viewed as a new and promising modeling avenue that permits to achieve more realistic service restoration plans.

TABLE IV
RESTORATION BENEFITS: VALUES OF Z^*, Z^{T*}, AND Z^{W*} FOR THE SINGLE-LINE DAMAGE SCENARIOS

IEEE 33-Node Test System					
Scenarios (S)	Z^*	Z^{T*}	Z^{W*}	Z^*-Z^{T*}	Z^*-Z^{W*}
S1	671023	669107	669742	1916	1281
S2	592340	584936	590824	7404	1516
S3	381717	380235	381380	1482	337
S4	356577	355055	356200	1522	377
IEEE 123-Node Test System					
Scenarios (S)	Z^*	Z^{T*}	Z^{W*}	Z^*-Z^{T*}	Z^*-Z^{W*}
S1	464104	461083	462055	3021	2049
S2	448216	445180	446166	3036	2050
S3	445201	442191	443178	3010	2023
S4	429938	426897	427655	3041	2283

TABLE V
RESTORATION BENEFITS: VALUES OF Z^*, Z^{T*}, AND Z^{W*} FOR THE STUDIED MULTI-LINE DAMAGE SCENARIOS

IEEE 33-Node Test System					
Scenarios (S)	Z^*	Z^{T*}	Z^{W*}	Z^*-Z^{T*}	Z^*-Z^{W*}
S1	661561	656992	657461	4569	4100
S2	348425	348187	348253	238	172
S3	637642	633543	634206	4099	3436
S4	447145	445903	446379	1242	766
S5	630886	612814	613578	18072	17308
S6	432418	402513	403468	29905	28950
IEEE 123-Node Test System					
Scenarios (S)	Z^*	Z^{T*}	Z^{W*}	Z^*-Z^{T*}	Z^*-Z^{W*}
S1	444985	444012	444353	973	632
S2	407722	407635	407674	87	48
S3	445032	444199	444640	833	392
S4	402162	402105	402138	57	24
S5	445071	443887	444395	1184	676
S6	429876	428452	428794	1424	1082

VI. CONCLUSION

This paper proposed a service restoration optimization model that utilizes MPSs for enhancing the DS resilience when facing extreme emergencies. We introduced the concept of node immediate restoration metric (IRM) to make optimal MPSs scheduling decisions to deliver resilience services. The IRM for each interrupted node depends on the travel and waiting times for an MPS to reach that node, and was thereby modeled as an endogenous source of uncertainty. The proposed problem takes the form of an MINLP optimization model. An efficient linearization method was designed to reformulate it as an equivalent MILP formulation, which can be solved faster and more efficiently. Extensive numerical results on two test systems and over a variety of outage scenarios clearly highlighted the benefits of the reformulation method and the efficacy of the proposed approach in boosting the power distribution network resilience against HILP extremes. Additionally, the value of endogenous uncertainty considerations in the use of MPSs for service restoration was quantified and compared with the traditional MPSs modeling approaches. The analyses of the results demonstrated that the traditional models overestimate the actual availability of the MPSs and the resilience benefits, while the proposed model capturing endogenous uncertainties offer a more realistic estimation of the MPSs contributions to DS resilience enhancement.

In general, knowledge on the intensity of an HILP event and the resulting damaged branches in the DS can significantly impact the optimal decisions on MPS deployment for resilience delivery in the network. While the focus of this paper was solely on modeling and assessment of endogenous uncertainties in the MPS availability for service restoration in the DS, future research could explore the problem with a stochastic programming formulation accounting also for external (exogenous) sources of uncertainty, including but not limited to the uncertain realization of the extreme event and damaged scenarios, intermittent renewable resources, and variable electrical demand. The explicit modeling and representation of such uncertainties would lead to the formulation of risk-averse stochastic programming problems including, for example, chance constraints or conditional value-at-risk constraints. Additionally, the proposed formulation with endogenous uncertainty can be used within a rolling horizon framework [5] that can supersede a larger-scale multi-period optimization solution process with a series of the proposed static optimization problems rolled over time.

REFERENCES

[1] S. Lei, C. Chen, H. Zhou, and Y. Hou, "Routing and scheduling of mobile power sources for distribution system resilience enhancement," *IEEE Trans. on Smart Grid*, vol. 10, no. 5, pp. 5650–5662, 2018.

[2] D. Barrett, "Few big FEMA generators humming," *Wall Street J.*, 2012.

[3] Z. Yang, P. Dehghanian, and M. Nazemi, "Seismic-resilient electric power distribution systems: Harnessing the mobility of power sources," *IEEE Trans. on Ind. Applications*, vol. 56, no. 3, pp. 2304–2313, 2020.

[4] S. Yao, T. Zhao, H. Zhang, P. Wang, and L. Goel, "Two-stage stochastic scheduling of transportable energy storage systems for resilient distribution systems," in *2018 IEEE International Conference on Probabilistic Methods Applied to Power Systems (PMAPS)*, pp. 1–6, IEEE, 2018.

[5] S. Yao, P. Wang, X. Liu, H. Zhang, and T. Zhao, "Rolling optimization of mobile energy storage fleets for resilient service restoration," *IEEE Transactions on Smart Grid*, vol. 11, no. 2, pp. 1030–1043, 2020.

[6] S. Lei, C. Chen, Y. Li, and Y. Hou, "Resilient disaster recovery logistics of distribution systems: Co-optimize service restoration with repair crew and mobile power source dispatch," *IEEE Trans. on Smart Grid*, vol. 10, no. 6, pp. 6187–6202, 2019.

[7] Z. Ye, C. Chen, B. Chen, and K. Wu, "Resilient service restoration for unbalanced distribution systems with DERs by leveraging mobile generators," *IEEE Trans. on Industr. Inform.*, pp. 1386–1396, 2020.

[8] S. Lei, J. Wang, C. Chen, and Y. Hou, "Mobile emergency generator pre-positioning and real-time allocation for resilient response to natural disasters," *IEEE Trans. Smart Grid*, vol. 9, no. 3, pp. 2030–2041, 2016.

[9] P. Prabawa and D. Choi, "Multi-agent framework for service restoration in distribution systems with distributed generators and static/mobile energy storage systems," *IEEE Access*, vol. 8, pp. 51736–51752, 2020.

[10] S. Yao, P. Wang, and T. Zhao, "Transportable energy storage for more resilient distribution systems with multiple microgrids," *IEEE Transactions on Smart Grid*, vol. 10, no. 3, pp. 3331–3341, 2019.

[11] Y. Xu, Y. Wang, J. He, M. Su, and P. Ni, "Resilience-oriented distribution system restoration considering mobile emergency resource dispatch in transportation system," *IEEE Access*, vol. 7, pp. 73899–73912, 2019.

[12] T. Ding, Z. Wang, W. Jia, B. Chen, C. Chen, and M. Shahidehpour, "Multiperiod distribution system restoration with routing repair crews, mobile electric vehicles, and soft-open-point networked microgrids," *IEEE Trans. on Smart Grid*, vol. 11, no. 6, pp. 4795–4808, 2020.

[13] L. Che and M. Shahidehpour, "Adaptive formation of microgrids with mobile emergency resources for critical service restoration in extreme conditions," *IEEE Trans. Power Syst.*, vol. 34, pp. 742–753, 2019.

[14] H. H. Abdeltawab and Y. A. I. Mohamed, "Mobile energy storage scheduling and operation in active distribution systems," *IEEE Transactions on Industrial Electronics*, vol. 64, no. 9, pp. 6828–6840, 2017.

[15] D. Anokhin, P. Dehghanian, M. A. Lejeune, and J. Su, "Mobility-as-a-service for resilience delivery in power distribution systems," *Production and Operations Management*, vol. 30, no. 8, pp. 2492–2521, 2021.

[16] J. Silvente, G. M. Kopanos, V. Dua, and L. G. Papageorgiou, "A rolling horizon approach for optimal management of microgrids under stochastic uncertainty," *Chemical Engineering Research and Design*, vol. 131, pp. 293–317, 2018.

[17] W. Yanan, W. Jiekang, and M. Xiaoming, "Intelligent scheduling optimization of seasonal CCHP system using rolling horizon hybrid optimization algorithm and matrix model framework," *IEEE Access*, vol. 6, pp. 75132–75142, 2018.

[18] D. E. Olivares, C. A. Cañizares, and M. Kazerani, "A centralized energy management system for isolated microgrids," *IEEE Transactions on Smart Grid*, vol. 5, no. 4, pp. 1864–1875, 2014.

[19] L. Ma, N. Liu, J. Zhang, and L. Wang, "Real-time rolling horizon energy management for the energy-hub-coordinated prosumer community from a cooperative perspective," *IEEE Transactions on Power Systems*, vol. 34, no. 2, pp. 1227–1242, 2019.

[20] C. Revelle and K. Hogan, "The maximum reliability location problem and α-reliable p-center problem: Derivatives of the probabilistic location set covering problem," *Ann. Oper. Res.*, vol. 18, pp. 155–173, 1989.

[21] L. Hellemo, B. Paul I., and A. Tomasgard, "Decision-dependent probabilities in stochastic programs with recourse," *Computational Management Science*, vol. 15, no. 3-4, pp. 369–395, 2018.

[22] T. W. Jonsbråten, R. J. Wets, and D. L. Woodruff, "A class of stochastic programs withdecision dependent random elements," *Annals of Operations Research*, vol. 82, pp. 83–106, 1998.

[23] S. H. Cho, H. Jang, T. Lee, and J. Turner, "Simultaneous location of trauma centers and helicopters for emergency medical service planning," *Operations Research*, vol. 62, no. 4, pp. 751–771, 2014.

[24] M. A. Lejeune and F. Margot, "Aeromedical battlefield evacuation under endogenous uncertainty in casualty delivery times," *Management Science*, vol. 64, no. 12, pp. 5481–5496, 2018.

[25] M. A. Lejeune, F. Margot, and A. Delgado de Oliveira, "Chance-constrained programming with decision-dependent uncertainty: A MEDEVAC application," *Working Paper*, 2020.

[26] O. Nohadani and K. Sharma, "Optimization under decision-dependent uncertainty," *SIAM J. on Opt.*, vol. 28, no. 2, pp. 1773–1795, 2018.

[27] N. Noyan, G. Rudolf, and M. Lejeune, "Distributionally robust optimization under a decision-dependent ambiguity set with applications to machine scheduling and humanitarian logistics," *INFORMS Journal on Computing*, vol. 34, no. 2, pp. 729–751, 2022.

[28] J. Zhang, H. Xu, and L. Zhang, "Quantitative stability analysis for distributionally robust optimization with moment constraints," *SIAM J. on Opt.*, vol. 26, no. 3, pp. 1855–1882, 2016.

[29] R. Aringhieri, M. Bruni, S. Khodaparasti, and J. van Essen, "Emergency medical services and beyond: Addressing new challenges through awide literature review," *Comp. & Operations Res.*, vol. 78, pp. 349–368, 2018.

[30] O. Berman and D. Krass, "Stochastic location models with congestion," in *Location science*, pp. 477–535, Springer, 2019.

[31] M. E. Baran and F. F. Wu, "Network reconfiguration in distribution systems for loss reduction and load balancing," *IEEE Power Engineering Review*, vol. 9, no. 4, pp. 101–102, 1989.

[32] A. Arif, S. Ma, Z. Wang, J. Wang, S. M. Ryan, and C. Chen, "Optimizing service restoration in distribution systems with uncertain repair time and demand," *IEEE Trans. Power Syst.*, vol. 33, no. 6, pp. 6828–6838, 2018.

[33] M. Lavorato, J. F. Franco, M. J. Rider, and R. Romero, "Imposing radiality constraints in distribution system optimization problems," *IEEE Transactions on Power Systems*, vol. 27, no. 1, pp. 172–180, 2012.

[34] R. A. Jabr, R. Singh, and B. C. Pal, "Minimum loss network reconfiguration using mixed-integer convex programming," *IEEE Transactions on Power Systems*, vol. 27, no. 2, pp. 1106–1115, 2012.

[35] J. Su, D. Anokhin, P. Dehghanian, and M. A. Lejeune, "On the use of mobile power sources in distribution networks under endogenous uncertainty." *Electronic Appendix*. Accessed: 2022. Available: https://blogs.gwu.edu/seas-payman-lab/files/2022/09/AppendixMPS.pdf.

[36] G. P. McCormick, "Computability of global solutions to factorable nonconvex programs: Part I—Convex underestimating problems," *Mathematical Programming*, vol. 10, no. 1, pp. 147–175, 1976.

[37] S. Lei, J. Wang, and Y. Hou, "Remote-controlled switch allocation enabling prompt restoration of distribution systems," *IEEE Transactions on Power Systems*, vol. 33, no. 3, pp. 3129–3142, 2017.

[38] M. Gendreau, G. Laporte, and F. Semet, "The maximal expected coverage relocation problem for emergency vehicles," *Journal of the Operational Research Society*, vol. 57, no. 1, pp. 22–28, 2006.

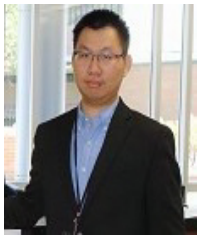

Jinshun Su (S'18) received B.Eng in electrical engineering from Xi'an University of Technology, China in 2017, and the M.Sc. degree in electrical engineering from The George Washington University, Washington, D.C., USA in 2019. He is currently pursuing the Ph.D. degree in electrical engineering at the Department of Electrical and Computer Engineering, The George Washington University, Washington, D.C., USA. His research interests include applications of mobile power sources, reliability and resiliency of smart grids.

Dmitry Anokhin received his BS and MS degrees in Applied Mathematics and Computer Science from Voronezh State University, Russia, in 2013, and the M.A. degree from Kent State University, USA, in 2016. From 2016 to 2018, he was a Lecturer at Kent State University, Ashtabula, USA, and California State University, Bakersfield, USA. Currently, he is pursuing his Ph.D. degree in the Department of Decision Sciences at the George Washington University School of Business in Washington, D.C. His research interests include data-driven risk-averse optimization models in the area of disaster management, power distribution systems, wildfires, and emergency healthcare.

Payman Dehghanian (S'11, M'17, SM'20) is an Assistant Professor at the Department of Electrical and Computer Engineering in George Washington University, Washington, D.C., USA. He received the B.Sc., M.Sc., and Ph.D. degrees all in Electrical Engineering respectively from University of Tehran, Tehran, Iran, in 2009, Sharif University of Technology, Tehran, Iran, in 2011, and Texas A&M University, Texas, USA in 2017. His research interests include power system reliability and resilience assessment, data-informed decision-making for maintenance and asset management in electrical systems, and smart electricity grid applications.

Dr. Dehghanian is the recipient of the 2014 and 2015 IEEE Region 5 Outstanding Professional Achievement Awards, the 2015 IEEE-HKN Outstanding Young Professional Award, the 2021 Early Career Award from the Washington Academy of Sciences, and the 2022 Early Career Researcher Award from the George Washington University.

Miguel Lejeune is a Full Professor of Decision Sciences (GWSB) and has a coutesy appointment in the Electrical and Computer Engineering (SEAS) at the George Washington University (GWU). Prior to joining GWU, he was a Visiting Assistant Professor in Operations Research at Carnegie Mellon University. He held visiting positions at Carnegie Mellon University, Georgetown University, the University of California – Irvine, and the Foundation Getulio Vargas in Rio de Janeiro. He is the recipient of the 2019 Koopman Award of the INFORMS Society, a CAREER/Young Investigator Research Grant from the Army Research Office, and the IBM Smarter Planet Faculty Innovation Award. Miguel Lejeune's areas of expertise include stochastic programming, distributionally robust optimization, and data-driven optimization with applications in finance, supply chain management, health care, and energy. His current research is funded by the National Science Foundation, the Office of Naval Research, and the DUKE Energy Innovation Fund.